Level Assignments in O^{17} from $C^{13}(\alpha,\alpha)C^{13}$ and $C^{13}(\alpha,n)O^{16}$†

B. K. Barnes, T. A. Belote,* and J. R. Risser
Bonner Nuclear Laboratories, Rice University, Houston, Texas
(Received 15 June 1965)

$C^{13}(\alpha,\alpha)C^{13}$ cross sections at center-of-mass angles 54.7°, 107.9°, 142.6°, and 169.6° and $C^{13}(\alpha,n)O^{16}$ cross sections at 0° have been measured at α-particle energies from 2 to 3.5 MeV. From dispersion-theory analysis, a consistent set of J^π and partial-width values has been obtained for eleven states of the compound nucleus O^{17} with excitation energies between 8 and 9 MeV.

I. INTRODUCTION

THE $C^{13}(\alpha,n)O^{16}$ reaction has been extensively investigated[1–5] at α-particle bombarding energies below 5 MeV. Resonances from sharp energy states of the compound nucleus O^{17} are observed. We have measured[6] the $C^{13}(\alpha,\alpha)C^{13}$ differential elastic-scattering cross sections for α-particle bombarding energies from 2.0 to 3.5 MeV at center-of-mass angles 54.7, 107.9, 142.6, and 169.6°. $C^{13}(\alpha,n)O^{16}$ differential reaction cross sections at 0° were measured simultaneously. Elastic-scattering and reaction data were analyzed to determine the J^π and the α-particle and neutron partial widths of the states of O^{17} corresponding to the observed resonances.

The range 2 to 3.5 MeV of α-particle bombarding energies corresponds to the range 7.9 to 9 MeV of excitation energies in the compound nucleus O^{17}. Values of J and of neutron and α-particle partial widths for many of the states at these excitation energies were known from $C^{13}(\alpha,n)O^{16}$ differential cross sections[2–5] and from total cross sections of O^{16} for neutrons.[2,5,7] From interference terms in $C^{13}(\alpha,n)O^{16}$ angular distributions,[4,5] relative parities of a number of states were known. To determine parities and to make complete determinations of J and partial-width values, $C^{13}(\alpha,\alpha)C^{13}$ and $O^{16}(n,n)O^{16}$ elastic-scattering experiments are necessary. The parameters of two states at the low end of the energy interval have recently been determined from analysis of $O^{16}(n,n)O^{16}$ angular distributions.[8]

II. EXPERIMENTAL PROCEDURE

The He^+ beam of the 5.5-MeV Van de Graaff accelerator was the source of the α particles. The energy scale was based on the $C^{13}(p,n)N^{13}$ thresholds at $E_p=3.236$ MeV and the $C^{13}(\alpha,n)O^{16}$ resonance at 2.800 MeV.[9] The scattering chamber has been described.[10,11] Solid-state detectors were used, and data were taken at two angles simultaneously.

The targets were thin self-supporting foils made from 41.6% C^{13}-enriched methyl iodide, or from 56.7% C^{13}-enriched methane, by a method previously described.[12] Mass-spectroscopic assays of the target material were obtained. Most of the targets were about 15 $\mu g/cm^2$ thick (about 23 keV for 2 MeV α particles); thinner targets proved too fragile. Target thickness was determined by measuring the number of protons elastically scattered from the target at a laboratory angle of 165° and a proton energy of 3.00 MeV with the counter solid angle and the integrated beam current used in the experiment.[13] This method of measuring target thickness has the advantage of basing the experimental $C^{13}(\alpha,\alpha)C^{13}$ cross sections only on the known proton differential elastic cross sections of C^{12} and C^{13} at this energy and angle (73.6 mb/sr for C^{12} and 68.6 mb/sr for C^{13}) and on the mass-spectroscopic value of the ratio of C^{13} to C^{12} in the target material.

Alpha particles scattered from C^{13} and from C^{12} could be resolved only at 169.6°, not at the other scattering angles. From the number of elastic α particles observed at each energy and angle, the number of α particles scattered from C^{12} had to be subtracted. The number scattered from C^{12} were calculated from the $C^{12}(\alpha,\alpha)C^{12}$ cross section and the C^{12} content of the target. The $C^{12}(\alpha,\alpha)C^{12}$ cross sections for each energy and angle were calculated: above 2.5 MeV from the phase shifts[14]; between 2.0 and 2.5 MeV by extrapolating to the 2-MeV Rutherford cross sections. The C^{12}

† Work supported in part by the U. S. Atomic Energy Commission.

* Present address: Department of Physics, Massachusetts Institute of Technology, Cambridge, Massachusetts.

[1] T. W. Bonner, A. A. Kraus, Jr., J. B. Marion, and J. P. Schiffer, Phys. Rev. **102**, 1348 (1956).

[2] R. L. Becker and H. H. Barschall, Phys. Rev. **102**, 1384 (1956).

[3] M. G. Rusbridge, Proc. Phys. Soc. (London) **A69**, 830 (1956).

[4] J. P. Schiffer, A. A. Kraus, Jr., and J. R. Risser, Phys. Rev. **105**, 1811 (1957).

[5] R. B. Walton, J. D. Clement, and F. Borelli, Phys. Rev. **107**, 1065 (1957).

[6] B. K. Barnes, R. L. Steele, T. A. Belote, and J. R. Risser, Bull. Am. Phys. Soc. **8**, 125 (1963).

[7] D. B. Fossan, R. L. Walter, W. E. Wilson, and H. H. Barschall, Phys. Rev. **123**, 209 (1961).

[8] C. H. Johnson and J. L. Fowler, paper to be presented at the International Conference on the Study of Nuclear Structure with Neutrons, Antwerp, Belgium, 1965, (unpublished) and private communication.

[9] J. B. Marion, Rev. Mod. Phys. **33**, 19, 623 (1961).

[10] E. Kashy, R. R. Perry, and J. R. Risser, Phys. Rev. **117** 1289 (1960).

[11] T. A. Belote, E. Kashy, and J. R. Risser, Phys. Rev. **122**, 920 (1961).

[12] E. Kashy, R. R. Perry, and J. R. Risser, Nucl. Instr. Methods **4**, 167 (1959).

[13] E. Kashy, R. R. Perry, R. L. Steele, and J. R. Risser, Phys. Rev. **122**, 884 (1961).

[14] C. Miller Jones, G. C. Phillips, R. W. Harris, and E. H. Beckner, Nucl. Phys. **37**, 1 (1962).

content of the target was calculated for each datum point from the original C^{12} content of the target plus the content of the C^{12} deposit built up by the α-particle beam. The C^{12} deposit was assumed to have been built up in equal increments per datum point, since the points were taken with the same integrated beam current and the beam was on the target only during the points. A target-thickness measurement with 3-MeV protons was made at the end of each run as well as at the beginning in order to obtain the total thickness of the C^{12} deposit.

The neutron yields from the $C^{13}(\alpha,n)O^{16}$ reaction were measured at 0° with a long counter at the same time the elastic scattering data were taken. The long counter subtended a cone of semi-apex angle 14°, corresponding to a laboratory solid angle of 0.19 sr. The counter was calibrated with a standard PuBe neutron source. Backgrounds from the beam tube and analyzing-magnet vacuum box were checked with the beam off the target.

III. ANALYSIS

For the states of the compound nucleus O^{17} below $E_x=9.44$ MeV, only two particle decay channels are open: neutron emission to the ground state of O^{16} and α-particle emission to the ground state of C^{13}. The sum of the partial width Γ_n for neutron emission to the ground state of O^{16} and Γ_α for α-particle emission to the ground state of C^{13} must therefore equal Γ, the total width of the state, since Γ_γ, the partial width for γ-ray emission, is negligible compared to Γ_n and Γ_α. In the $C^{13}+\alpha$ channel, since the C^{13} ground state is a $\frac{1}{2}^-$ state, the channel spin is $\frac{1}{2}$ and the parity $(-)^{l+1}$. In the $O^{16}+n$ channel, the channel spin is $\frac{1}{2}$ and the parity $(-)^{l'}$. For a state of even (odd) parity, l is odd (even) and l' even (odd). Parity of an isolated state can not be determined from a $C^{13}(\alpha,n)O^{16}$ angular distribution, because the angular distribution for l even and l' odd is the same as the angular distribution for l odd and l' even.

Elastic Scattering

Fits to the elastic data were calculated using dispersion theory with the single-level form of the S matrix given by Eq. (5.6) of Blatt and Biedenharn.[15] The differential elastic-scattering cross section for charged particles with channel spin $\frac{1}{2}$ is well known. The expression programmed for IBM 709 and 7094 computers is given by Eq. (1) of Belote, Kashy, and Risser.[11] The hard-sphere phases were put into the program as quadratic expressions, $\phi_l=A_l+B_lE+C_lE^2$, with E in MeV. The values of the coefficients used in the final elastic fits are given in Table I.

Resonance shapes from isolated states formed with $l\leqslant 4$ are shown in Fig. 1. The curves shown clearly that

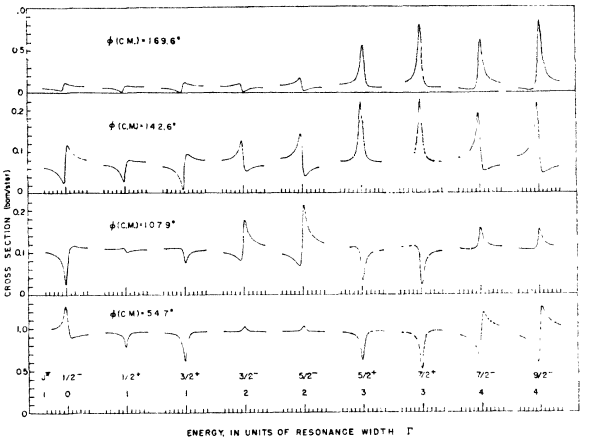

FIG. 1. $C^{13}(\alpha,\alpha)C^{13}$ resonance shapes from isolated states formed with $l\leqslant 4$.

l and therefore the parity determines the shape of the resonance. Shapes for all J^π were calculated as guides in choosing parameters in the early stages of the analysis.

$C^{13}(\alpha,n)O^{16}$

Fits to the experimental $C^{13}(\alpha,n)O^{16}$ differential cross section at 0° were calculated using an expression for differential reaction cross sections involving the S matrix and Z coefficients obtained from Eqs. (4.5), (4.6), and (5.6) of Blatt and Biedenharn.[15] The expression programmed for IBM 704, 709, and 7094 computers is given by Eq. (2) of Kashy, Perry, and Risser[10] with $i=0$, $I=\frac{1}{2}$, and with $S=S'=\frac{1}{2}$ only. This expression, while used to calculate differential cross sections at 0° as a function of energy, is an expression for calculating angular distributions, and the computer output contained the coefficients A_L of Legendre polynomials $P_L(\cos\theta)$ of angular distributions predicted by the nuclear parameters used in the calculations. Comparison with A_L values obtained from experimental $C^{13}(\alpha,n)O^{16}$ angular distributions[4,5] furnished an additional check on the choice of parameters.

The values of ϕ_l for the $O^{16}+n$ channel used in the calculations were: $\phi_0=-185°$; $\phi_1=-50°$; $\phi_2=-5°$; $\phi_l=0°$ for $l\geqslant 3$. The partial widths in the elastic and reaction cross sections were chosen to satisfy the condition $\Gamma_n/\Gamma+\Gamma_\alpha/\Gamma=1$. At places it was necessary to accept minor compromises in both elastic and reaction fits to satisfy the condition on the partial widths, but

TABLE I. Coefficients in $\phi_l=A_lE^2+B_lE+C_l$ used in the final fits to the elastic data. E is in MeV. $\phi_2=\phi_3=0$ for $E<2.5$ MeV. $\phi_l=0$ for $l>3$.

l	A_l	B_l	C_l	E
0	−2.52	1.19	−2.08	2–3.4
1	−2.67	1.33	−1.93	2–3.4
2	−1.49	6.79	−7.67	2.5–3.4
3	−4.39	1.92	−2.09	2.5–3.4

[15] J. M. Blatt and L. C. Biedenharn, Rev. Mod. Phys. **24**, 258 (1952).

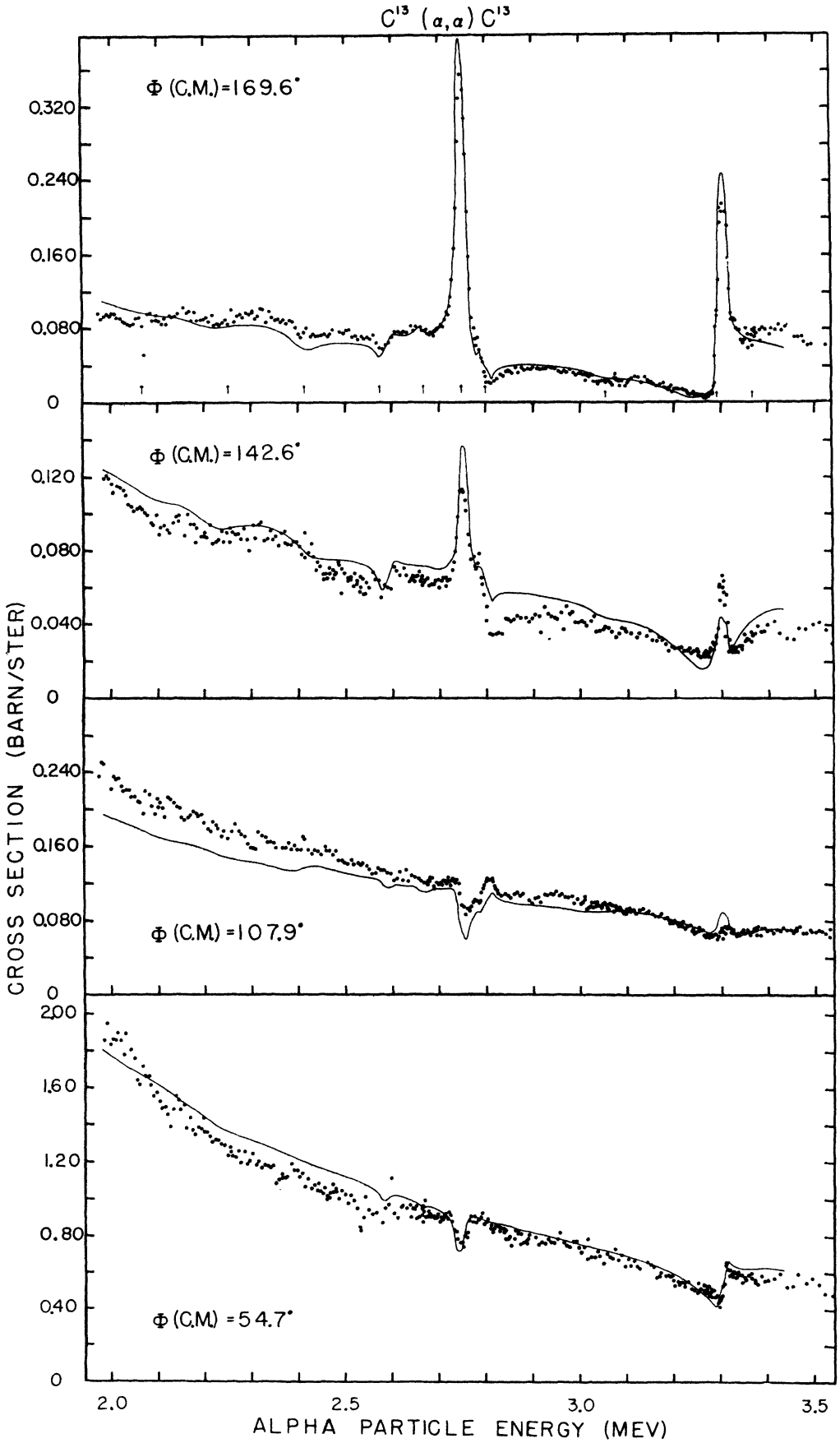

FIG. 2. Experimental $C^{13}(\alpha,\alpha)C^{13}$ center-of-mass differential cross sections at center-of-mass angles 54.7°, 107.9°, 142.6°, and 169.6°. The curves are the calculated fits with the parameters listed in Table II.

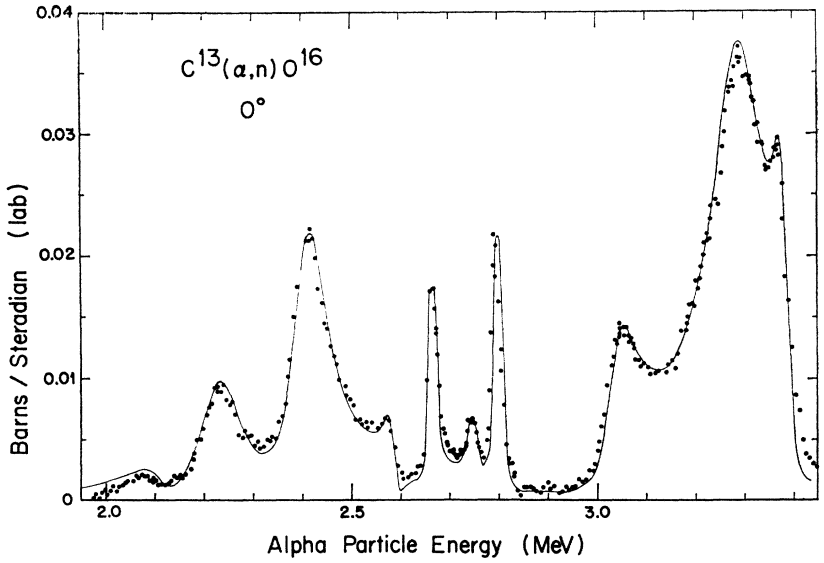

FIG. 3. Experimental $C^{13}(\alpha,n)O^{16}$ laboratory differential cross sections at 0°. The curve is the calculated fit with the parameters listed in Table II.

the final partial widths which gave satisfactory fits to both scattering and reaction data actually differed very little from values which gave the best fit to either set of data independently.

Since the self-supporting targets were thick ($\gtrsim 20$ keV for 2 MeV α particles) compared to some of the resonance widths, the cross sections were first calculated in fine energy steps as if the targets were thin compared to the widths, and then averaged over energy intervals equal to target thickness. In fitting the neutron data, the calculated cross sections were also averaged over the solid angle subtended by the long counter.

IV. EXPERIMENTAL RESULTS

$C^{13}(\alpha,\alpha)C^{13}$

The experimental center-of-mass elastic differential cross sections at center-of-mass angles 54.7, 107.9, 142.6, and 169.6° are shown in Fig. 2. Uncertainties in the absolute values of the cross sections are mainly due to the C^{12}-background subtraction. They are estimated to be less than $\pm 20\%$. Relative variations in the cross sections of much less than 20% over the resonances are significant, however, since the $C^{12}(\alpha,\alpha)C^{12}$ cross sections vary slowly with energy. In the region of low cross sections from 3 to 3.3 MeV at 169.6°, the number of particles scattered from C^{13} was taken directly from the pulse-height distributions, and the errors in these cross sections are estimated to be less than $\pm 30\%$. The energies are laboratory energies midway through the target. The curves are the calculated fits. Of the two strong resonances seen in the $C^{13}(\alpha,\alpha)C^{13}$ cross sections, at 2.750 and 3.305 MeV, the one at 3.305 MeV is not seen in $C^{13}(\alpha,n)O^{16}$. The parities of the states in O^{17} responsible for these two resonances (even parity from $l=3$ at 2.750 MeV; odd parity from $l=4$ at 3.305 MeV) can be directly inferred from comparisons of the resonance shapes in Fig. 2 with the single-level shapes of Fig. 1.

$C^{13}(\alpha,n)O^{16}$

The experimental $C^{13}(\alpha,n)O^{16}$ laboratory differential reaction cross sections at 0°, measured at the same time with the same targets and beam energies as the $C^{13}(\alpha,\alpha)C^{13}$ cross sections, are shown in Fig. 3. Uncertainties in the absolute cross sections are mainly due to the uncertainty in the calibration of the long counter. They are estimated to be less than $\pm 15\%$. The cross sections agree within experimental error with values previously published[2,5] except at the narrow resonances, where the peak cross sections depend on target thickness. The energies are laboratory energies midway through the target. The curve is the calculated fit.

V. PARAMETERS OF THE FITS

The values of the parameters used in the fits to the elastic and reaction data are listed in Table II. The resonance energies E_0 and widths Γ in the table are the

TABLE II. The values of the parameters used in the fits to the elastic and reaction data. ($\Gamma_n/\Gamma=1-\Gamma_\alpha/\Gamma$).

E_0 (MeV)	Γ_{lab} (keV)	Γ_α/Γ	J^π	E_x (MeV)	γ_α(% Wigner limit)	Γ_n(% Wigner limit)
2.110	90	0.03	$\frac{1}{2}^-$	7.970	1.08	0.75
2.233	110	0.05	$\frac{3}{2}^+$	8.064	2.78	1.09
2.407	84	0.11	$\frac{3}{2}^-$	8.197	8.23	1.27
2.583	11	0.44	$\frac{1}{2}^+$	8.332	1.13	0.06
2.663	7	0.08	$\frac{5}{2}^+$	8.393	1.13	0.30
2.750	10	0.97	$\frac{7}{2}^+$	8.460	15.63	0.01
2.800	6.7	0.26	$\frac{5}{2}^-$	8.498	0.74	0.07
3.037	68	0.06	$\frac{3}{2}^-$	8.679	0.98	0.82
3.290	130	0.50	$\frac{3}{2}^+$	8.873	5.52	0.51
3.305	8	1.00	$\frac{7}{2}^-$	8.884	20.71	0.00
3.385	30	0.04	$\frac{7}{2}^-$	8.945	2.62	5.75

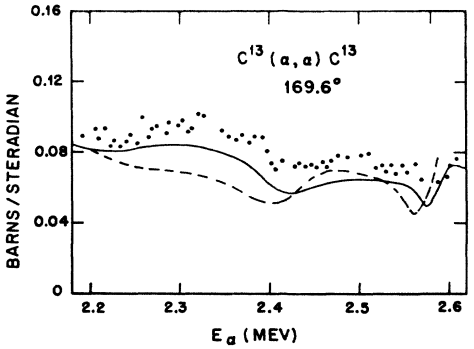

FIG. 4. Comparison of the fits from the assignments $\frac{1}{2}^+$, $\frac{3}{2}^-$, $\frac{3}{2}^+$ (dashed curve) and $\frac{1}{2}^-$, $\frac{3}{2}^+$, $\frac{3}{2}^-$ (solid curve) at the 2.110-, 2.233-, and 2.407-MeV resonances to the experimental $C^{13}(\alpha,\alpha)C^{13}$ data at 169.6° c.m. The assignment is $\frac{1}{2}^+$ at the 2.583-MeV resonance for both cases.

values put into the computer program to obtain thin-target cross sections, which were then averaged over target thickness to obtain the curves of Figs. 2 and 3. Differences between the values of E_0 in Table II and previously published values[1,4,5] are in part due to our use of the 2.800-MeV resonance as an energy calibration point[9,16] and in part to the fact that peaks in the differential cross sections do not occur precisely at the energies E_0 in cases of strong interference. The widths Γ at the 2.663- and 2.800-MeV resonances were measured by the thick target yield method using the $C^{13}(\alpha,n)O^{16}$ reaction. The values so obtained, 7.0±2 keV and 6.7±2 keV, respectively, are in better agreement with the values of Bonner, Kraus, Marion, and Schiffer[1] and of Williamson, Katman, and Burton[16] than with those of Walton, Clement, and Borelli.[5]

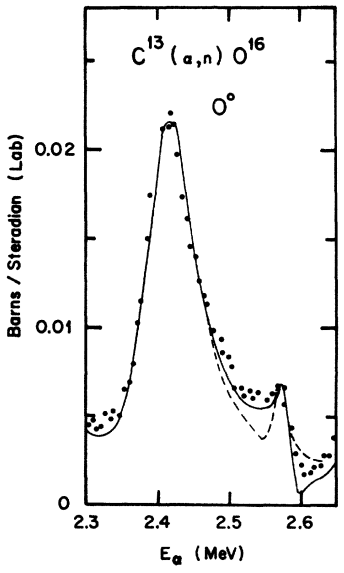

FIG. 5. Comparison of the fits from the assignments $\frac{1}{2}^+$ (solid curve) and $\frac{1}{2}^-$ (dashed curve) at the 2.583-MeV resonance to the experimental 0° $C^{13}(\alpha,n)O^{16}$ cross sections. The assignment at the 2.407-MeV resonance is $\frac{3}{2}^-$ in both cases.

[16] R. M. Williamson, T. Katman, and B. S. Burton, Phys. Rev. 117, 1325 (1960).

Considerations in the choice of the J^π values of Table II are discussed at some length in the following section. Also listed in Table II are the excitation energies of the states of O^{17} corresponding to the resonances and the neutron and α-particle reduced widths of the states expressed in percent of the Wigner limit.

VI. DISCUSSION OF J^π ASSIGNMENTS

Since the values of Γ_α/Γ are small at many of the resonances, final choices between possible assignments depend on detailed comparisons of calculated and experimental scattering and reaction cross sections. Examples of differences in detail between the best fits obtained with alternate J^π choices are discussed in the following paragraphs.

The parity was known to alternate[4,5] between the 2.110-, 2.233-, and 2.407-MeV resonances and the J values were known[4,5,7] to be $\frac{1}{2}$, $\frac{3}{2}$, and $\frac{3}{2}$, respectively. In Fig. 4, which shows the $C^{13}(\alpha,\alpha)C^{13}$ 169.6° cross sections from 2.2 to 2.6 MeV, the dashed curve corresponds to the choice $\frac{1}{2}^+$, $\frac{3}{2}^-$, $\frac{3}{2}^+$ and the solid curve to the choice $\frac{1}{2}^-$, $\frac{3}{2}^+$, and $\frac{3}{2}^-$. While the differences are not great, the solid curve reproduces the relative cross sections better.

From analysis of experimental $O^{16}(n,n)O^{16}$ angular distributions, Johnson, and Fowler[8] make $J^\pi=\frac{1}{2}^-$ and $\frac{3}{2}^+$ assignments to states in O^{17} showing as neutron resonances at 4.05 and 4.2 MeV, neutron energies which correspond to the 2.110- and 2.233-MeV resonances in $C^{13}(\alpha,n)O^{16}$, in agreement with our assignments.

In Fig. 5, which shows the $C^{13}(\alpha,n)O^{16}$ differential cross sections at 0° from 2.3 to 2.65 MeV, the dashed curve corresponds to the assignment $J^\pi=\frac{1}{2}^-$ at 2.583 MeV and the solid curve to $J^\pi=\frac{1}{2}^+$. For both curves the assignment is $\frac{1}{2}^-$, $\frac{3}{2}^+$, and $\frac{3}{2}^-$ at the 2.110-, 2.233-, and 2.407-MeV resonances.

Figures 6 and 7 show fits from several alternative assignments in the region of the narrow 2.663-, 2.750-, and 2.800-MeV resonances. Relative parity assign-

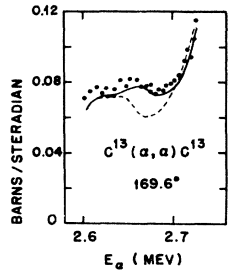

FIG. 6. Two fits to the elastic data at 169.6° c.m. with $J=\frac{7}{2}^+$ at the 2.750-MeV resonance and with alternative assignments at the 2.663-MeV resonance: $J=\frac{5}{2}^-$ (dashed curve) and $J=\frac{5}{2}^+$ (solid curve). The assignment at the 2.800-MeV resonance is $\frac{5}{2}^-$ in both cases.

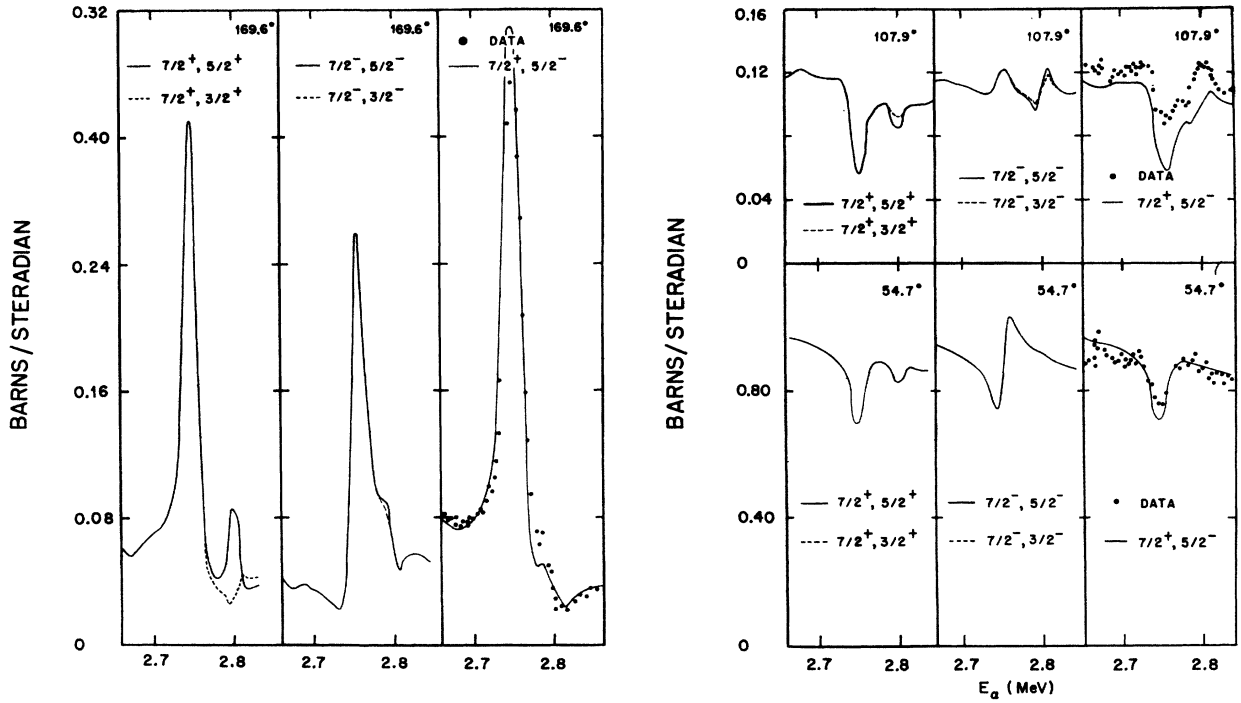

FIG. 7. The elastic data between 2.7 and 2.8 MeV at c.m. angles 54.7°, 107.9°, and 169.6° c.m. compared with fits from several assignments at the 2.750- and 2.800-MeV resonances. The experimental points were repeated many times and the data always showed the detail at 2.78 MeV at 107.9° and 169.6° c.m. The only fit reproducing this detail is the fit with $\frac{7}{2}^+$ at 2.750 MeV and $\frac{5}{2}^-$ at 2.800 MeV.

ments in this region are significant because the 2.750-MeV resonance is strong in the $C^{13}(\alpha,\alpha)C^{13}$ cross sections and the corresponding state can be assigned a definite parity. The state is formed with $l=3$ α particles, as is evident from a comparison of the shapes at 2.750 MeV in the elastic cross sections of Fig. 2 with the single-level resonance shapes of Fig. 1. Of the two possible J values reached with $l=3$, the higher value $J=\frac{7}{2}$ is required by the magnitudes of the cross sections in both $C^{13}(\alpha,\alpha)C^{13}$ and $C^{13}(\alpha,n)O^{16}$. Figure 6 shows two fits to the elastic data at 169.6° with $J^\pi=\frac{7}{2}^+$ at 2.750 and with alternative parity assignments at 2.663 MeV: $\frac{5}{2}^-$ (dashed curve) and $\frac{5}{2}^+$ (solid curve). The solid curve fits the data better. Figure 7 shows several alternatives at the 2.800-MeV resonance. The combination $\frac{7}{2}^+$, $\frac{5}{2}^-$ at the 2.750- and 2.800-MeV resonances fits the elastic data best at all angles. The combination $\frac{7}{2}^+$, $\frac{3}{2}^+$ (Ref. 5) can be rejected by comparison with the data between 2.75 and 2.80 MeV at 169.6° and 107.9°. Data in this energy interval at these angles was taken many times and always showed the same details: (1) a steep drop, a slight break, then another steep drop at 169.6°; (2) a small notch part way up the rise at 107.9°. The assignment $J=\frac{3}{2}$ at 2.800 results in a smaller calculated $C^{13}(\alpha,n)O^{16}$ cross section on resonance than is observed, even with $\Gamma_a=\Gamma_n=\Gamma/2$. If Γ is smaller than 6.7 keV, as the value 4 keV obtained by Williamson *et al.*[16] may indicate, the magnitude of the $C^{13}(\alpha,n)O^{16}$ cross section on the 2.800-MeV resonance would definitely rule out a $\frac{3}{2}$ assignment.

For the three overlapping resonances seen in $C^{13}(\alpha,n)O^{16}$ at 3.037, 3.290, and 3.385 MeV, the parities were known to alternate[4,5] and J values of $\frac{3}{2}$, $\frac{3}{2}$, and $\frac{7}{2}$

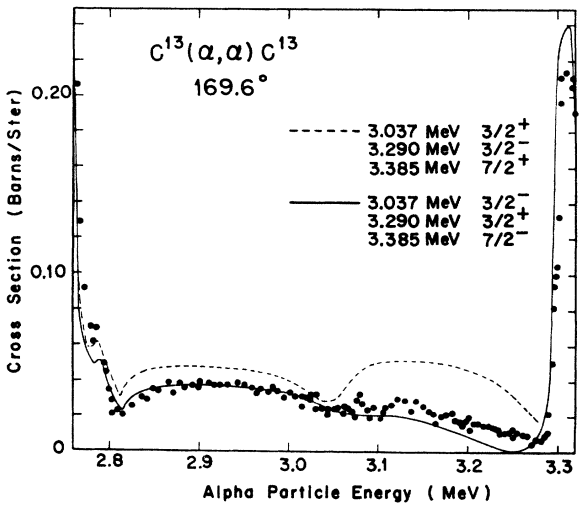

FIG. 8. Comparison of the fits from the assignments $\frac{3}{2}^+$, $\frac{3}{2}^-$, $\frac{7}{2}^+$ (dashed curve) and $\frac{3}{2}^-$, $\frac{3}{2}^+$, $\frac{7}{2}^-$ (solid curve) at the 3.037-, 3.290-, and 3.385-MeV resonances to the elastic data at 169.6°. The assignments at 2.750 and 2.800 MeV are $\frac{7}{2}^+$ and $\frac{5}{2}^-$ for both cases.

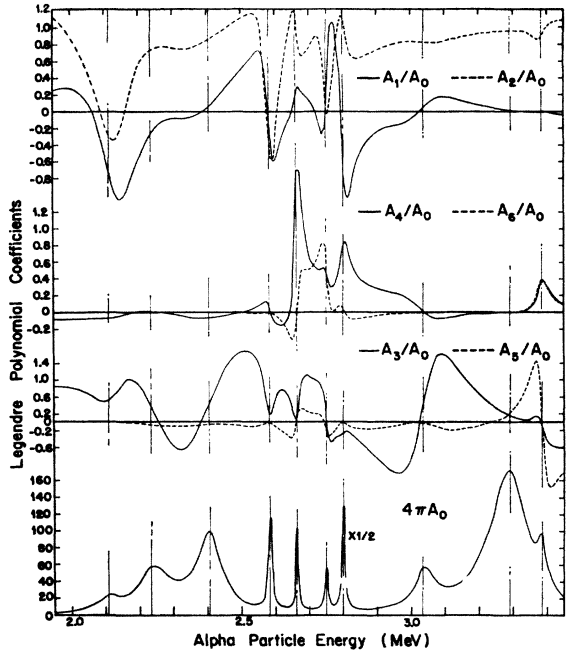

FIG. 9. The coefficients A_L of Legendre polynomial expansions of $C^{13}(\alpha,n)O^{16}$ angular distributions predicted by the parameters of Table II. The ratios A_L/A_0 are plotted versus α-particle bombarding energy. The total $C^{13}(\alpha,n)O^{16}$ cross section $4\pi A_0$ predicted by the parameters of Table II are plotted below.

were assigned.[2,4,5,7] Figure 8 shows the fits to the 169.6° elastic data for the two parity choices. For both fits the assignments at 2.750 and 2.800 MeV were $J^\pi=\frac{7}{2}^+$ and $\frac{5}{2}^-$, respectively. In the region of low cross sections from 3 to 3.3 MeV at 169.6°, the number of α-particles scattered from C^{13} were taken directly from the pulse-height distributions and the errors in the cross sections are estimated to be less than $\pm 30\%$. The discrepancies between the dashed curve and the data points are therefore greater than the experimental errors in the data. The solid curve corresponding to the assignment $\frac{3}{2}^-$, $\frac{3}{2}^+$, and $\frac{7}{2}^-$ at 3.037, 3.290, and 3.385 MeV, respectively, fits the data very well.

The J^π assignments and other parameters of Table II can be further checked against experiment by comparing predicted $C^{13}(\alpha,n)O^{16}$ angular distributions with those obtained experimentally.[4,5] Figure 9 is a plot of values of A_L/A_0, where the A_L are coefficients in Legendre-polynomial expansions of $C^{13}(\alpha,n)O^{16}$ angular distributions, calculated from the parameters of Table II. These can be compared with a similar plot of values of A_L/A_0 obtained from least squares fits to experimental angular distributions by Walton, Clement, and Borelli[5] (Fig. 6, p. 1070). The agreement is quite good considering the fact that experimental uncertainties are reflected in both sets of coefficients and that the angular distributions of Walton *et al.*[5] were taken with targets about 20 keV thick while the A_L/A_0 of Fig. 9 were not averaged over an energy interval equivalent to a target thickness. Comparisons for A_L/A_0 with $L\geqslant 4$ are probably the most significant. The agreement for A_6/A_0 between 2.6 and 2.8 MeV is a strong argument for the correctness of the assignments $J=\frac{5}{2}$ and $\frac{7}{2}$ with like parity at 2.663 and 2.750 MeV and $J<\frac{5}{2}$ or opposite parity at 2.800 MeV. It is also an argument for the parity choices made at the 3.037-, 3.290- and 3.385-MeV resonances. Choice of a positive parity for the $\frac{7}{2}$ state corresponding to the 3.385-MeV resonance was found to have a marked effect on A_6/A_0 between 2.6 and 2.8 MeV and to make the agreement with experiment considerably less satisfactory. A parameter which is much more significant in the calculation of the A_L/A_0 than of the $C^{13}(\alpha,n)O^{16}$ cross sections is the sign of either $\sqrt{\Gamma_\alpha}$ or $\sqrt{\Gamma_n}$. A fairly systematic investigation of the effect of sign reversals was made. Negative signs for $\sqrt{\Gamma_n}$ (or $\sqrt{\Gamma_\alpha}$) at 2.233 and 3.385 MeV were used to obtain the curves of Fig. 9.

VII. CONCLUSIONS

Since the values of Γ_α/Γ are small at many of the resonances which are strong in the $C^{13}(\alpha,n)O^{16}$ reaction cross sections and the values of Γ_n/Γ small at several which are strong in the $C^{13}(\alpha,\alpha)C^{13}$ cross sections, assignments depend in many cases on detailed comparison between predicted and experimental cross sections. The parameters given in Table II for the states of the compound nucleus O^{17} are consistent with all the evidence from the $C^{13}(\alpha,\alpha)C^{13}$ cross sections, the $C^{13}(\alpha,n)O^{16}$ cross sections at 0° and $C^{13}(\alpha,n)O^{16}$ angular distribution data.